

# RSC Advances



This is an *Accepted Manuscript*, which has been through the Royal Society of Chemistry peer review process and has been accepted for publication.

*Accepted Manuscripts* are published online shortly after acceptance, before technical editing, formatting and proof reading. Using this free service, authors can make their results available to the community, in citable form, before we publish the edited article. This *Accepted Manuscript* will be replaced by the edited, formatted and paginated article as soon as this is available.

You can find more information about *Accepted Manuscripts* in the [Information for Authors](#).

Please note that technical editing may introduce minor changes to the text and/or graphics, which may alter content. The journal's standard [Terms & Conditions](#) and the [Ethical guidelines](#) still apply. In no event shall the Royal Society of Chemistry be held responsible for any errors or omissions in this *Accepted Manuscript* or any consequences arising from the use of any information it contains.

# Neutral Au<sub>n</sub> (n=3-10) Cluster Catalyzes Acetylene Hydrochlorination: A Density Functional Theory Study

Yang Wang, Mingyuan Zhu, Lihua Kang\*, Bin Dai\*

College of Chemistry and Chemical Engineering/ Key Laboratory for Green Processing of Chemical Engineering of Xinjiang Bingtuan. Shihezi University, Shihezi, Xinjiang, 832000, PR China

**Abstract:** The mechanisms of acetylene hydrochlorination to vinyl chloride catalyzed by neutral Au<sub>3-10</sub> cluster were systematically investigated using density functional theory with B3LYP/LANL2DZ function. In this reaction, the gold cluster functions as a bridge of electron transfer: the electrons transfer from C<sub>2</sub>H<sub>2</sub> to the gold cluster then from the gold cluster to HCl. HCl and C<sub>2</sub>H<sub>2</sub> are simultaneously activated by the gold cluster, which presents a synergistic effect in co-adsorption. In the size range of Au<sub>3</sub> to Au<sub>10</sub>, all gold clusters undergo the same catalytic cycle. The whole process of the acetylene hydrochlorination on the gold cluster consists of two transition states and one intermediate, and the dissociation of hydrogen chloride is the rate-controlling step. Overall, small-sized gold clusters perform better than large-sized clusters, and the odd-number atom clusters are better than even-number atom clusters.

**Keywords:** neutral gold acetylene hydrochlorination DFT mechanism

\*Corresponding author. E-mail: [kanglihua@shzu.edu.cn](mailto:kanglihua@shzu.edu.cn)

Tel: +86-0993-2057213;

Fax: +86-0993-2057270

## 1. Introduction

Interest in gold catalysis has been increasing, and the subject is now well-established in both heterogeneously and homogeneously catalyzed reactions.<sup>1-6</sup> Gold, in its bulk form, is known to possess little or no catalytic activity. However, small gold clusters exhibit remarkably different fundamental properties. An increasing number of studies have shown that gold clusters with appropriate sizes show considerably good activity for various catalytic reactions.<sup>7-30</sup> For example, nanosized gold clusters exhibit a high catalytic activity toward carbon monoxide oxidation,<sup>8,17,18,19</sup> selective oxidation of olefin and alcohol,<sup>10,11</sup> water-gas shift reaction,<sup>12,14</sup> synthesis of hydrogen peroxide,<sup>13</sup> S-H bond rupture of thiophenol and mercaptan,<sup>20,21</sup> acetylene hydrogenation,<sup>16</sup> and acetylene hydrochlorination.<sup>7,9,15,26-30</sup> Among various reactions catalyzed by gold clusters, acetylene hydrochlorination has received the most attention because of its considerable economic benefits, wide range of industrial applications, and huge potential for improvement.

In 1985, Hutchings et al. predicted that supported gold catalyst may be a substitute for mercuric chloride as the more “green material” for the hydrochlorination of acetylene.<sup>7</sup> Since then, AuCl<sub>3</sub> was found to be the best catalyst for acetylene hydrochlorination from among 30 carbon-supported metal chlorides.<sup>23</sup> In 2013, L. Kang et al. studied the reaction mechanism of C<sub>2</sub>H<sub>3</sub>Cl over an MCl<sub>x</sub> (M = Hg, Au, Ru; x=2, 3) catalyst, and they confirmed the conclusion theoretically.<sup>24</sup> However, AuCl<sub>3</sub> catalyst was unstable due to deactivation, and J. Zhang et al. have studied the deactivation mechanism over AuCl<sub>3</sub> dimer model catalyst using DFT.<sup>25</sup> In

2014, M. Zhu and his coworkers developed different methods to inhibit the deactivation of Au<sup>3+</sup> like adding 1, 10-phenanthroline or polypyrrole (PPy) into AuCl<sub>3</sub> catalyst.<sup>26-29</sup> Given the improvement in catalyst preparation, A. Corma et al. reported a method to prepare isolated gold atoms supported on functionalized carbon nanotubes,<sup>21</sup> which shows that the ultra-fine nanoparticle is not only limited in theoretical research. A. Corma et al. found that single gold atoms are not active, but they aggregate under reaction conditions into gold clusters of low atomicity that exhibit a catalytic activity comparable to that of sulfhydryl oxidase enzymes. When clusters grow into larger nanoparticles, catalyst activity drops to zero. To improve the utilization efficiency of Au catalyst for the reduction of 4-nitrophenol, X. Jia et al. prepared triangular Au nanoplates on functional reduced graphene oxide by a facile method. The products with ultra-low trace amounts of Au afforded high catalytic efficiency.<sup>22</sup> Even though numerous studies have shown that properly sized nano-gold clusters exhibit high catalytic activities for various reactions,<sup>7-22</sup> no investigations have been conducted thus far on the acetylene hydrochlorination reaction by using neutral gold catalysts. We believe that theoretical calculations should precede experimental investigations and provide direction for experimental studies. The precise control of the crystal plane and cluster size of gold nanoparticles in experiments is difficult, but controlling these parameters is easily achievable in theoretical calculations.

In this paper, we present a DFT study on the acetylene hydrochlorination of a neutral Au cluster in an attempt to answer the following questions: (1) Where and how

are HCl and C<sub>2</sub>H<sub>2</sub> activated on an Au cluster? (2) Where and how does acetylene hydrochlorination occur? (3) What is the catalytic function of the Au cluster? Several possible reaction pathways are explored with the aim of unraveling the details of acetylene hydrochlorination on an Au<sub>n</sub> cluster. We predict that a deep understanding of these details will be important in this field of study.

## 2. Computational methods

All density functional calculations were performed using the Gaussian09 program package.<sup>31</sup> No geometric constraints were assumed in geometry optimization. All structures containing Au were optimized and characterized at B3LYP/LANL2DZ. The nonlocal correlation functional of Lee, Yang, and Parr<sup>32</sup> (B3LYP) with the 6-31++G\*\* basis set was used for H, C, and Cl atoms,<sup>33</sup> and the Los Alamos effective core pseudo-potentials (ECP) basis set LANL2DZ was used for the Au atoms. All reported charges are Mulliken local charges (Au). The relative energies of the reactants, products, intermediates, and transition states presented in this study were zero-point-energy (ZPE) obtained from frequency calculations at the same level of optimization. All stationary points were characterized as the minima (no imaginary frequency) or transition state (one imaginary frequency) via Hessian calculation. Intrinsic reaction coordinate (IRC) calculations<sup>34,35</sup> were performed to determine if each transition state links the correct product with the reactant. Basis set superposition error (BSSE) corrections evaluated by the counterpoise method<sup>36</sup> were taken into account.

Through the frontier molecular orbital (FMO) and charge distribution analysis, we

can determine the approximate distribution of the active sites of the  $Au_n$  cluster, and the highest occupied molecular orbital (HOMO) and lowest unoccupied molecular orbital (LUMO) energies of the neutral  $Au_n$  clusters,  $C_2H_2$ , and HCl were theoretically calculated at the B3LYP/LANL2DZ. We then calculated the HOMO–LUMO energy gaps as two groups, namely, between HOMO (gold clusters) and LUMO ( $C_2H_2$ /HCl), and between LUMO (gold clusters) and HOMO ( $C_2H_2$ /HCl). We obtained the lowest HOMO–LUMO energy gaps and confirmed the electron donor and acceptor. Thus, we can know which FMO factors prominently in the adsorption processes. Besides, through the charge distribution analysis of isolated cluster and molecules in the adsorbed complexes, that can further verify the predicted result of FMO analysis, which makes our results be more persuasive and reliable.

An important reference point for this calculation is the adsorption energy for HCl and  $C_2H_2$  adsorbed on isolated  $Au_n$  clusters. In this paper, we used the following definitions for adsorption energy.

When HCl or  $C_2H_2$  is adsorbed on isolated Au, the adsorption energy is calculated as:

$$E = E_{(\text{system})} - E_{(\text{Au})} - E_{(\text{HCl}/C_2H_2)}$$

When HCl is adsorbed on Au- $C_2H_2$ , the adsorption energy is calculated as:

$$E = E_{(\text{system})} - E_{(\text{Au}-C_2H_2)} - E_{(\text{HCl})}$$

When  $C_2H_2$  is adsorbed on Au-HCl, the adsorption energy is calculated as:

$$E = E_{(\text{system})} - E_{(\text{Au}-\text{HCl})} - E_{(C_2H_2)}$$

$E_{(\text{system})}$  is the total energy of adsorption system;  $E_{(\text{Au}-C_2H_2)}$  and  $E_{(\text{Au}-\text{HCl})}$  denote the

energy of the Au complexes that absorbs  $C_2H_2$  and HCl, respectively.

### 3. Results and Discussion

#### 3.1 Co-adsorption of $C_2H_2$ and HCl on $Au_n$ ( $n=3-10$ ) clusters.

In Fig. S3, we compared the energy gaps of HOMO–LUMO ( $HCl \rightarrow Au_n$ ) and HOMO–LUMO ( $C_2H_2 \rightarrow Au_n$ ) and yielded the following two main results: 1) for both HCl and  $C_2H_2$ , the energy gaps of even-numbered  $Au_n$  clusters are larger than those on adjacent odd-numbered ones, and 2) overall, the energy gaps of HOMO–LUMO ( $HCl \rightarrow Au_n$ ) are larger than those of HOMO–LUMO ( $C_2H_2 \rightarrow Au_n$ ) for even-numbered ones. The energy gaps denote the ability of the electrons to transfer between HCl/ $C_2H_2$  and  $Au_n$  clusters. To explore the electronic properties and the interactions between  $Au_n-C_2H_2$  complexes and HCl, we calculated the FMO and corresponding orbital energies of the  $Au_n-C_2H_2$  complexes, as shown in Fig. 1. In Table 1, we listed the orbital energies of the LUMO and HOMO of HCl and  $Au_n-C_2H_2$  and their different energy gaps. The energy gaps of HOMO–LUMO ( $Au_n-C_2H_2 \rightarrow HCl$ ) are smaller than those of HOMO–LUMO ( $HCl \rightarrow Au_n-C_2H_2$ ). This result indicates that  $Au_n-C_2H_2$  complexes are electron donors and HCl is an electron acceptor. The electrons transfer from the HOMO of  $Au_n-C_2H_2$  complexes (almost from the  $Au_n$  clusters) to the LUMO of HCl. Therefore, we can preliminarily predict the distribution of reaction sites from the HOMO of  $Au_n-C_2H_2$  complexes in Fig. 1. The following points are noted:  $Au_{3-5}-C_2H_2$  complexes only have one adsorption site for HCl;  $Au_7-C_2H_2$  complex has two adsorption sites, namely, Au (1) and Au (4) atoms (the code numbers of Au clusters are shown in Fig. S1); in  $Au_{6,8,9}-C_2H_2$  complexes,

the three co-adsorption configurations are different from the others because  $C_2H_2$  was adsorbed vertically on  $Au_{6,8,9}$ . Their adsorption sites are a block of void that comprised three Au atoms. For example, the adsorption void of the  $Au_{6,8}-C_2H_2$  complex is composed of Au (1), Au (2), and Au (4), whereas that of the  $Au_9-C_2H_2$  complex consists of Au (3), Au (2), and Au (5).

In Fig. 2, the configuration of  $Au_{3,5,7,10}-C_2H_2-HCl$  complexes is planar, whereas that of  $Au_{4,6,8,9}-C_2H_2-HCl$  complexes is in the form of stereo structures. The adsorption energies of HCl on  $Au_n-C_2H_2$  ( $n = 4, 6, 8, 9$ ) complexes approximate each other. The catalytic mechanism of acetylene hydrochlorination involves facilitating the dissociation of the H-Cl and  $C\equiv C$  bonds. Therefore, the catalyst's ability to weaken the strong H-Cl and  $C\equiv C$  bonds and the degree of this weakening are crucial factors that affect its catalytic activity towards acetylene hydrochlorination. The bond lengths of HCl and  $C_2H_2$  are all effectively lengthened in the  $Au_n-C_2H_2-HCl$  complexes. The bond length increase (%) of  $R_{C=C}$  ( $C_2H_2$ ) and  $R_{H-Cl}$  (HCl) in  $Au_n-C_2H_2-HCl$  complexes are listed in table 2. In Fig. 3, all the studied  $Au_n$  clusters have varying degrees of activation toward  $C_2H_2$  and HCl. The weakening degree of HCl is generally stronger than that of  $C_2H_2$  in  $Au_n-C_2H_2-HCl$  complexes. The bond length of HCl in  $Au_5-HCl$  is the most obvious and that of  $Au_{6,8}-HCl$  are not obvious. In Fig. S3, we found that the values of  $Au_6$  and  $Au_8$  coordinate points locate at peak. According to Fig. 3 and Fig. S3, we can conclude that acetylene adsorption is better on gold clusters than on hydrogen chloride, and both bond lengthening upon adsorption and HOMO-LUMO gaps consistently indicate the highest activation for

Au<sub>5</sub> and the lowest one for Au<sub>6</sub> and Au<sub>8</sub>.

### 3.2 Mechanisms of acetylene hydrochlorination catalyzed by neutral Au<sub>n</sub> (n=3–10) clusters

In the size range of Au<sub>3</sub> to Au<sub>10</sub>, all gold clusters undergo the same catalytic cycle, as shown in Fig. 4. The whole process of acetylene hydrochlorination in Au<sub>n</sub> (n=3-10) clusters does not vary across all clusters. However, the catalytic performances are different because of different sizes and active sites of the gold clusters. In Fig. 5, the difference in the energies of transition states and intermediates is evident. The path diagram shows two energy barriers, i.e., for the dissociation of hydrogen chloride and the transfer of proton from the Au cluster to chloroethenyl. The energies of acetylene adducts of the Au<sub>6</sub>, Au<sub>8</sub>, Au<sub>9</sub> clusters are extremely low such that the second energy barrier is apparently higher than those of the others. We conjectured that this observation may be connected with their special structures (Fig. 6). If HCl is absorbed in the special triangle void, the proton of HCl would have difficulty in migrating out of the space.

It is worthy of note that, by comparing the HOMO of Au<sub>6,8,9</sub>-C<sub>2</sub>H<sub>2</sub> in Fig. 6, we found that the HOMO distributions were round the special block of void comprised of three Au atoms. But the HOMO of Au<sub>9</sub>-C<sub>2</sub>H<sub>2</sub> seems a little different from the other two cases. We have studied the “odd–even” effect of the gold cluster (Fig. S3, in supporting information), which the even- and odd-numbered clusters are different in terms of their electronic performances. So we think that the difference of HOMO between Au<sub>9</sub>-C<sub>2</sub>H<sub>2</sub> and Au<sub>6,8</sub>-C<sub>2</sub>H<sub>2</sub> may be related to the “odd–even” effect of the

gold cluster. After all, the “odd–even” effect is ubiquitous and plays a role in Au<sub>3-10</sub> clusters.

### 3.2.1 Coplanarity of C<sub>2</sub>H<sub>2</sub> and HCl on Au<sub>3, 5, 7, 10</sub> clusters.

For the Au<sub>3,5,7,10</sub> clusters, C<sub>2</sub>H<sub>2</sub> and HCl are coplanar with the gold clusters, as seen in Fig. 7. Why do we compare Au<sub>10</sub> with Au<sub>3,5,7</sub> instead of Au<sub>9</sub>? Based on the “odd–even” effect of the gold cluster (Fig. S3, in supporting information), the even- and odd-numbered clusters are different in terms of their catalytic performance. In Fig. S2 (in supporting information), the HOMO–Au<sub>5</sub> and HOMO–Au<sub>10</sub> indicate that Au<sub>5</sub> and Au<sub>10</sub> have similar bridge active sites. In Fig. 7, the Ts1 of Au<sub>3,5,7,10</sub> clusters indicate the dissociation processes of HCl, and the dissociation is a synergistic effect under the Au atom and C<sub>2</sub>H<sub>2</sub>. In im1, the proton and chloroethenyl occupy both ends of the bridge active sites, and the chloroethenyl plane occurs a 90-degree flip. The 90-degree flip is an important configuration adjustment, which can effectively reduce the steric hindrance during proton transfer. In Ts2, the proton of HCl transfers from the Au site to chloroethenyl, and the energy barrier is considerably lowered after the configuration adjustment of chloroethenyl. This reaction is generally an exothermic process with an energy of 29.1 kcal mol<sup>-1</sup>. The reaction occurs easily on gold clusters because the liberated heat can sufficiently offset the activation energy during the dissociation processes of HCl. Moreover, vinyl chloride is desorbed from the gold cluster, that is, the small-size Au cluster is a highly effective catalyst. Among the Au<sub>3,5,7,10</sub> clusters, the activation energy of Au<sub>5</sub> is the lowest (21.2 kcal mol<sup>-1</sup>) because of its highly active bridge site.

### 3.2.2 Skew-planar of C<sub>2</sub>H<sub>2</sub> and HCl on Au<sub>4,6,8,9</sub> clusters.

The co-adsorption of HCl and C<sub>2</sub>H<sub>2</sub> on the gold clusters varies and may affect the reaction because of the different structures and electron distributions of the gold clusters. In Fig. 8, we listed the energy diagrams of acetylene hydrochlorination pathways on the Au<sub>4,6,8,9</sub> clusters. Comparison with Fig. 7 demonstrates their apparent difference. Two strong peaks are found in the energy diagrams of the Au<sub>4,6,8,9</sub> clusters, whereas one strong peak occurs on the Au<sub>3,5,7,10</sub> clusters. In Co-ads, HCl and C<sub>2</sub>H<sub>2</sub> are adsorbed at the skew-planar of the Au<sub>4,6,8,9</sub> clusters, especially on the Au<sub>6,8,9</sub> clusters. Meanwhile, HCl is adsorbed above the gold cluster and C<sub>2</sub>H<sub>2</sub> is adsorbed at the top site of the gold cluster (in Fig. 6). In Ts1, a marked deformation occurs in the Au<sub>4</sub> cluster, which stretches the cluster and reduces the total energy of the system. The activation energy decreases to 15.3 kcal mol<sup>-1</sup>, but the Au<sub>4</sub> cluster is restored to its original state in Im1. In the second energy barrier (from Im1 to Ts2), the rates decrease in the following order: Au<sub>6</sub> > Au<sub>9</sub> > Au<sub>8</sub> > Au<sub>4</sub>. This order is related to the size of the special block of void of HOMO distributions in Au<sub>6,8,9</sub>-C<sub>2</sub>H<sub>2</sub> (Fig. 6). Bigger special blocks of void of HOMO distributions lead to adsorption of HCl and thus increase difficulty in the process of proton transfer from the triangular domain. Aside from these effects, the proton and chloroethenyl are adsorbed at the same gold atom in Ts2, which is different from the Ts2 in the Au<sub>5,7</sub> clusters. For the Au<sub>6</sub> cluster, the rate-controlling step is the transfer of the proton from the Au cluster to chloroethenyl instead of the dissociation of HCl. By comparing the two groups, the catalytic performances of the Au<sub>3,5,7,10</sub> clusters are better than those of the Au<sub>4,6,8,9</sub>

clusters. Therefore, the small-sized gold clusters result in a higher catalytic performance than large-sized clusters, and odd-number atom clusters perform better than even-number atom clusters. These results also verified the speculation in Fig. S3 (in supporting information).

### 3.2.3 The correlation between electronic property and activation energy.

In Fig. 9, we found that there was a direct relationship between the energy gaps of HOMO-LUMO ( $\text{Au}_n\text{-C}_2\text{H}_2\rightarrow\text{HCl}$ ) and activation energies. The red line also follows the “odd–even” effect of the gold cluster like the black line (Fig. S3, in supporting information). However, there are a little differences at  $\text{Au}_4$  and  $\text{Au}_9$  coordinate points. Why the activation energy of  $\text{Au}_4$  and  $\text{Au}_9$  occur exception in red line? We think that the decrease of activation energy of  $\text{Au}_4$  cluster may be concerned with the abnormal configuration of  $\text{Ts}_2$  in  $\text{Au}_4$  cluster. In all the configurations of  $\text{Ts}$  (transient state) and  $\text{Im}$  (intermediate) of  $\text{Au}_{3-10}$  clusters, the  $\text{Ts}_1$  of  $\text{Au}_4$  cluster is the only one which occurs deformation (Fig. 8). In  $\text{Ts}_1$ , this marked deformation stretches the size of cluster and reduces the total energy of  $\text{Ts}_1$ . Thereby, this variation reduces the energy barrier between Co-ads and  $\text{Ts}_1$  of  $\text{Au}_4$ . So in the red line, there is an abnormal decrease of activation energy at  $\text{Au}_4$  coordinate point. As for  $\text{Au}_9$  cluster, the exception may be concerned with its special structure (Fig. 6). The special block of void comprised of three Au atoms in  $\text{Au}_9$  is very similar to the  $\text{Au}_6$  and  $\text{Au}_8$ , which maybe result in the increase of activation energy like  $\text{Au}_6$  and  $\text{Au}_8$  and deviating the “odd–even” rule.

In conclusion, there is a direct relationship between the energy gaps of

HOMO-LUMO ( $Au_n-C_2H_2 \rightarrow HCl$ ) and activation energies indeed. However  $Au_4$  and  $Au_9$  don't follow the "odd-even" rule, those may be concerned with their special structures, and thus also support our conclusion in return. That is, we believe that apart from the size of gold clusters, different types of active sites or configurations can affect the catalytic activity performance.

In the end, by comparing with reference of J. Hutchings et al.,<sup>15</sup> we found that this reaction could be achieved by forming active reaction species  $C_2H_2-AuCl_3-HCl$ , which is similar to  $C_2H_2-Au_n-HCl$ . Besides, they also concluded that the dissociation of hydrogen chloride was the rate-controlling step, and the activation energy barrier was  $23.5 \text{ kcal mol}^{-1}$ . That indicates the gold-base catalysts are consistent in mechanism of acetylene hydrochlorination generally, but the catalytic performance has certain difference. By improving process of preparing and ultra-fine gold clusters of low atomicity, the acetylene hydrochlorination can be achieved in a higher efficiency with ultra-low trace amounts of Au catalyst.

#### 4. Conclusion

Two different types of active sites exist in the Au clusters, namely, the top and bridge sites. In the  $Au_{4,6,8,9}$  clusters, HCl and  $C_2H_2$  are activated by the top sites, whereas activation in the  $Au_{3,5,7,10}$  clusters occurs in bridge sites. In the co-adsorption process,  $Au_n-C_2H_2$  complexes are electron donors and HCl is an electron acceptor, which indicates that electrons transfer from the HOMO of  $Au_n-C_2H_2$  complexes (almost from  $Au_n$  clusters) to the LUMO of HCl. Thus, the gold cluster functions as a bridge for electron transfer.

The whole process of the acetylene hydrochlorination in the gold clusters involves two transition states (Ts1 and Ts2) and one intermediate (Im1). The process of Ts1 denotes the dissociation of HCl, whereas Ts2 refers to the proton transfer from the Au cluster to chloroethenyl. On the whole, the small-sized gold clusters result in a higher catalytic performance than large-sized clusters, and odd-number atom clusters perform better than even-number atom clusters. There is a direct relationship between the energy gaps of HOMO-LUMO ( $Au_n-C_2H_2 \rightarrow HCl$ ) and activation energies indeed. We believe that apart from the size of gold clusters, different types of active sites or configurations can affect the catalytic activity performance.

### Acknowledgements

We gratefully acknowledge the financial supports for the Special Funds for Major State Basic Research Program of China (No. 2012CB720302), the National Natural Science Foundation of China (NSFC, Grant No. 21363020) and the Ph.D. Programs Foundation of the Xinjiang Production and Construction Corps (No. 2013BB010).

### References and Notes

- 1 G. J. Hutchings, *Catal. Today*, 2005, **100**, 55-61.
- 2 A. S. K. Hashmi and G. J. Hutchings, *Angew. Chem. Int. Ed.*, 2006, **45**, 7896-7936.
- 3 Z. Li, C. Brouwer and C. He, *Chem. Rev.*, 2008, **108**, 3239-3265.
- 4 R. Sardar, A. M. Funston, P. Mulvaney and R. W. Murray, *Langmuir*, 2009, **25**, 13840-13851.
- 5 C. H. Christensen and J. K. Norskov, *Science*, 2010, **327**, 278-279.
- 6 A. Corma, A. Leyva-Pérez and M. J. Sabater, *Chem. Rev.*, 2011, **111**, 1657-1712.

- 7 G. J. Hutchings, *J. Catal.*, 1985, **96**, 292-295.
- 8 M. Haruta, N. Yamada, T. Kobayashi and S. Iijima, *J. Catal.*, 1989, **115**, 301-309.
- 9 G. J. Hutchings, *Gold. Bull.*, 1996, **29**, 123-130.
- 10 J. E. Bailie and G. J. Hutchings, *Chem. Commun.*, 1999, 2151-2152.
- 11 P. Landon, P. J. Collier, A. J. Papworth, C. J. Kiely and G. J. Hutchings, *Chem. Commun.*, 2002, 2058-2059.
- 12 Q. Fu, H. Saltsburg and M. Flytzani-Stephanopoulos, *Science*, 2003, **301**, 935-939.
- 13 M. D. Hughes, Y. Xu, P. Jenkins, P. McMorn, P. Landon, D. I. Enache, A. F. Carley, G. A. Attard, G. J. Hutchings, F. King, E. H. Stitt, P. Johnston, K. Griffin and C. J. Kiely, *Nature*, 2005, **437**, 1132-1135.
- 14 F. Shi, X. Li, Y. Xia, L. Zhang and Z. Yu, *J. Am. Chem. Soc.*, 2007, **129**, 15503-15512.
- 15 M. Conte, A. F. Carley, C. Heirene, D. J. Willock, P. Johnston, A. A. Herzing, C. J. Kiely and G. J. Hutchings, *J. Catal.*, 2007, **250**, 231-239.
- 16 B. Yang, R. Burch, C. Hardacre, G. Headdock and P. Hu, *ACS Catal.*, 2012, **2**, 1027-1032.
- 17 H. Y. Kim, H. M. Lee and G. Henkelman, *J. Am. Chem. Soc.*, 2012, **134**, 1560-1570.
- 18 J. Lu, C. Aydin, N. D. Browning and B. C. Gates, *Angew. Chem.*, 2012, **124**, 5944-5948.
- 19 C. Liu, Y. Tan, S. Lin, H. Li, X. Wu, L. Li, Y. Pei and X. Zeng, *J. Am. Chem. Soc.*,

- 2013, **135**, 2583–2595.
- 20 A. P. Woodham, G. Meijer and A. Fielicke, *J. Am. Chem. Soc.*, 2013, **135**, 1727–1730.
- 21 A. Corma, P. Concepcion, M. Boronat, M. J. Sabater, J. Navas, M. J. Yacaman, E. Larios, A. Posadas, M. A. Lopez-Quintela, D. Buceta, E. Mendoza, G. Guilera and A. Mayoral, *Nature chem.*, 2013, **5**, 775–781.
- 22 W. Wang, J. Gu, W. Hua, X. Jia and K. Xi, *Chem. Commun.*, 2014, doi: 10.1039/c4cc03306j.
- 23 B. Nkosi, N. J. Coville and G. J. Hutchings, *J. Chem. Soc. Chem. Commun.*, 1988, 71–72.
- 24 M. Zhu, L. Kang, Y. Su, S. Zhang and B. Dai, *Can. J. Chem.*, 2013, **91**, 120–125.
- 25 J. Zhang, Z. He, W. Li and Y. Han, *RSC Adv.*, 2012, **2**, 4814–4821.
- 26 C. Huang, M. Zhu, L. Kang and B. Dai, *Catal. Commun.*, 2014, doi: 10.1016/j.catcom.2014.05.024.
- 27 C. Huang, M. Zhu, L. Kang, X. Li and B. Dai, *Chem. Eng. J.*, 2014, **242**, 69–75.
- 28 X. Li, M. Zhu and B. Dai, *Appl. Catal. B-Environ.*, 2013, **142–143**, 234–240.
- 29 X. Li, Y. Wang, L. Kang, M. Zhu, B. Dai, *J. Catal.*, 2014, **311**, 288–294.
- 30 X. Li, X. Pan, L. Yu, P. Ren, X. Wu, L. Sun, F. Jiao and X. Bao, *Nat. Commun.*, 2014, doi: 10.1038/ncomms4688.
- 31 M. J. Frisch, G. W. Trucks, H. B. Schlegel, G. E. Scuseria, M. A. Robb, J. R. Cheeseman, G. Scalmani, V. Barone, B. Mennucci, G. A. Petersson, H. Nakatsuji, M. Caricato, X. Li, H. P. Hratchian, A. F. Izmaylov, J. Bloino, G. Zheng, J. L. Sonnenberg, M. Hada, M. Ehara, K. Toyota, R. Fukuda, J. Hasegawa, M. Ishida, T. Nakajima, Y. Honda, O. Kitao, H. Nakai, T. Vreven, J. A. Montgomery Jr., J. E.

Peralta, F. Ogliaro, M. Bearpark, J. J. Heyd, E. Brothers, K. N. Kudin, V. N. Staroverov, R. Kobayashi, J. Normand, K. Raghavachari, A. Rendell, J. C. Burant, S. S. Iyengar, J. Tomasi, M. Cossi, N. Rega, J. M. Millam, M. Klene, J. E. Knox, J. B. Cross, V. Bakken, C. Adamo, J. Jaramillo, R. Gomperts, R. E. Stratmann, O. Yazyev, A. J. Austin, R. Cammi, C. Pomelli, J. W. Ochterski, R. L. Martin, K. Morokuma, V. G. Zakrzewski, G. A. Voth, P. Salvador, J. J. Dannenberg, S. Dapprich, A. D. Daniels, Ö. Farkas, J. B. Foresman, J. V. Ortiz, J. Cioslowski and D. J. Fox, Gaussian 09, Gaussian, Inc., Wallingford CT, 2010.

32 C. Lee, W. Yang and R. G. Parr, *Phys. Rev. B*, 1988, **37**, 785-789.

33 M. Andersson and P. Uvdal, *J. Phys. Chem. A*, 2005, **109**, 2937–2941.

34 C. Gonzalez and H. B. Schlegel, *J. Phys. Chem. C*, 1989, **90**, 2154-2162.

35 C. Gonzalez and H. B. Schlegel, *J. Phys. Chem. C*, 1990, **94**, 5523-5527.

36 F. B. Vanduijneldt, J. G. C. M. V. vande Rijdt and J. H. Lenthe, *Chem. Rev.*, 1994, **94**, 1873 –1885.

## Figure Captions

- Fig. 1. Frontier molecular orbitals and corresponding orbital energies of the  $Au_n-C_2H_2$  ( $n=3-10$ ) calculated at the B3LYP/LANL2DZ level of theory. (energies in eV, isovalue = 0.02)
- Fig. 2. The optimal co-adsorption configurations and adsorption energies of HCl on different  $Au_n-C_2H_2$  complexes. (The bond length in Å and energies in kcal mol<sup>-1</sup>)
- Fig. 3. The variation of bond length increase (%) of  $R_{C\equiv C}$  ( $C_2H_2$ ) and  $R_{H-Cl}$  (HCl) in  $Au_n-C_2H_2-HCl$  complexes.
- Fig. 4. The catalytic cycle of acetylene hydrochlorination catalyzed by gold clusters.
- Fig. 5. The energy diagrams of the most favorable pathways of acetylene hydrochlorination on  $Au_n$  ( $n=3-10$ ) clusters: reactants (Re), co-adsorbed reactants (Co-ads), transition states (Ts), intermediate (Im), desorption products (De-Pr) and products (Pr). The data are zero-point-energy (ZPE) in kcal mol<sup>-1</sup>.
- Fig. 6. The special block of void comprised of three Au atoms in  $Au_{6,8,9}-C_2H_2$  and corresponding HOMO distributions.
- Fig. 7. Energy diagrams of the most favorable pathways of acetylene hydrochlorination on  $Au_{3,5,7,10}$  clusters: reactants (R), co-adsorbed reactants (Co-ads), transition states (Ts), intermediate (Im), desorption products (De-Pr) and products (Pr). The data are zero-point-energy (ZPE) in kcal mol<sup>-1</sup>.
- Fig. 8. Energy diagrams of the most favorable pathways of acetylene hydrochlorination on  $Au_{4,6,8,9}$  clusters: reactants (R), co-adsorbed reactants

(Co-ads), transition states (Ts), intermediate (Im), desorption products (De-Pr) and products (Pr). The data are zero-point-energy (ZPE) in kcal mol<sup>-1</sup>.

Fig. 9. The correlation between energy gaps and activation energies. The black line denotes energy gaps of HOMO-LUMO ( $\text{Au}_n\text{-C}_2\text{H}_2 \rightarrow \text{HCl}$ ); The red line denotes the activation energy in the catalytic cycle of acetylene hydrochlorination.

Fig. 1

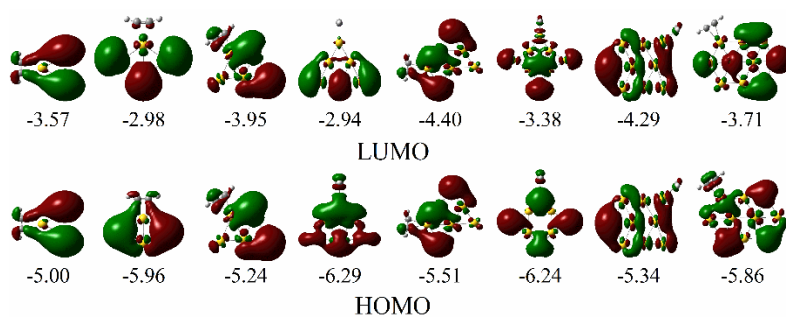


Fig. 2

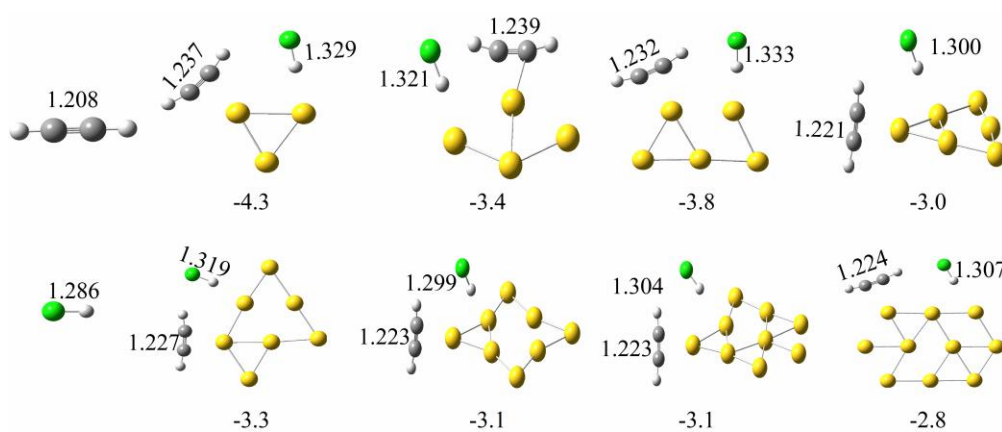


Fig. 3

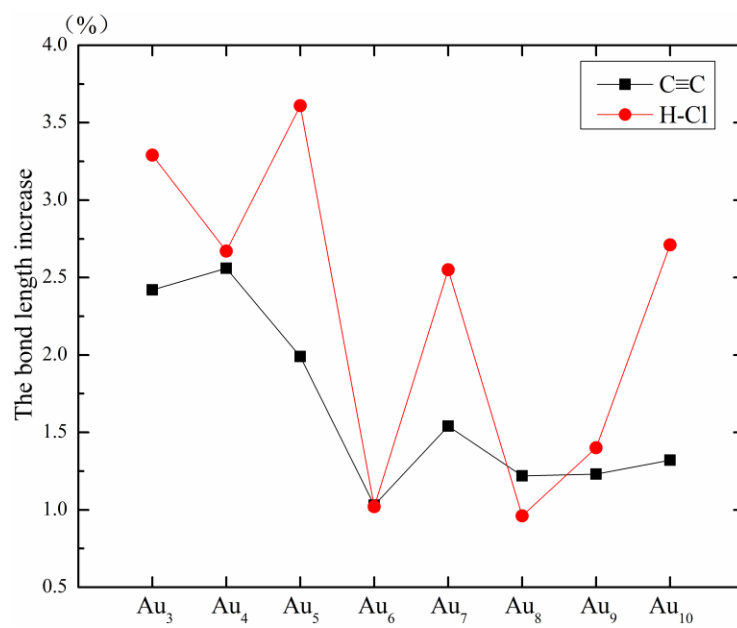


Fig. 4

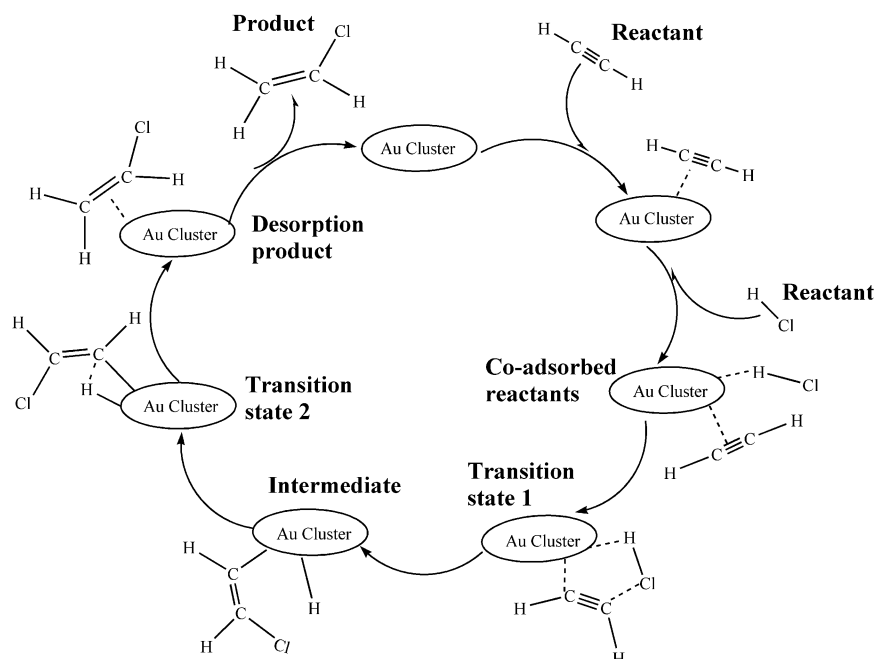


Fig. 5

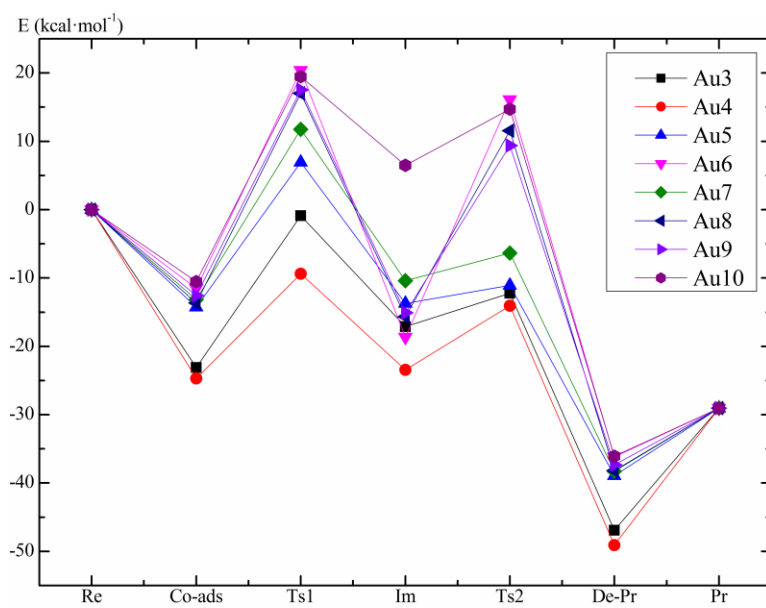


Fig. 6

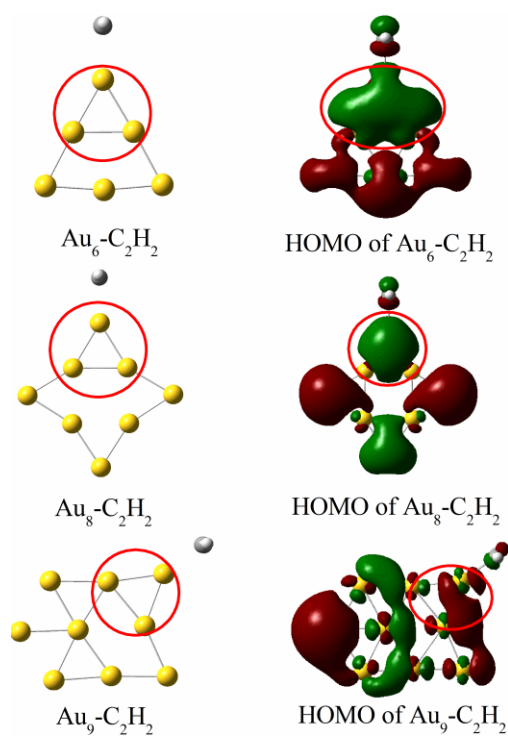


Fig. 7

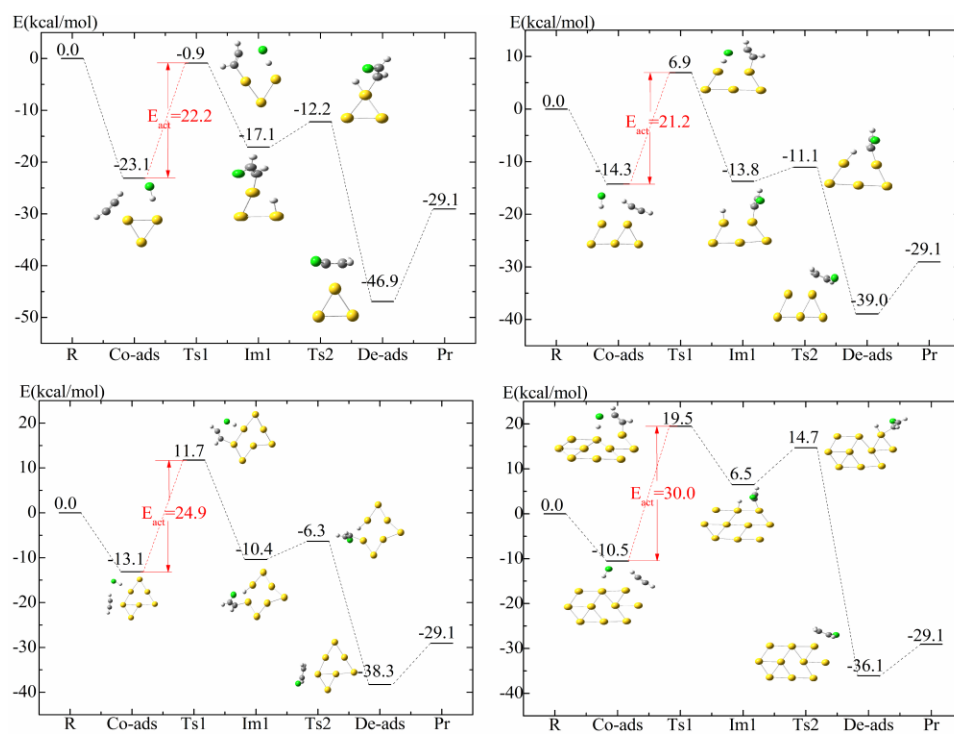


Fig. 8

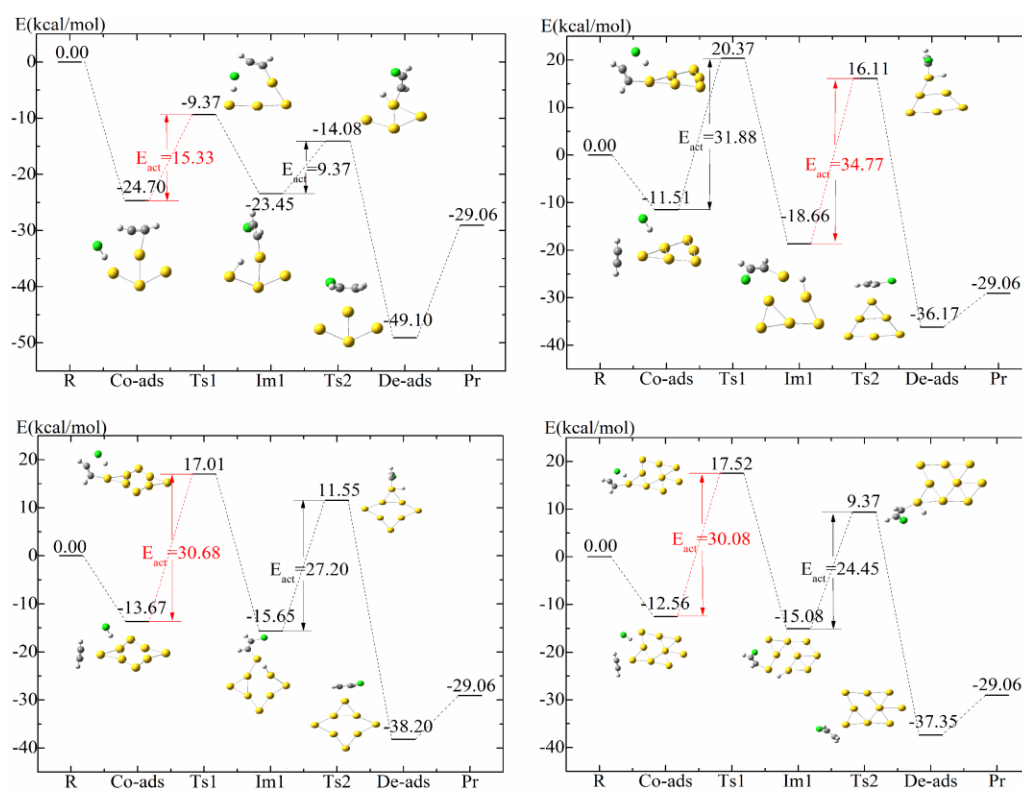


Fig. 9

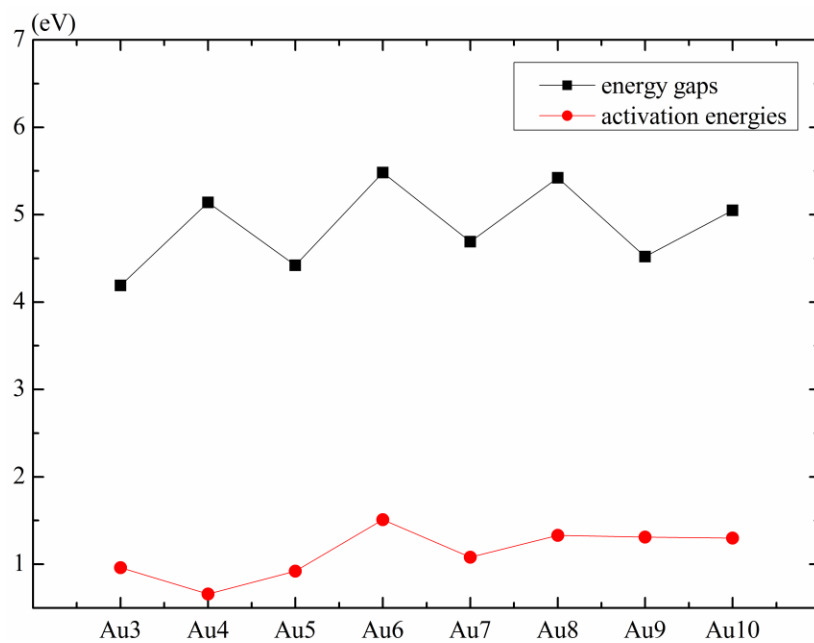


Table 1. The orbital energies on LUMO and HOMO of HCl and Au<sub>n</sub>-C<sub>2</sub>H<sub>2</sub>, and their different energy gaps between HCl and Au<sub>n</sub>-C<sub>2</sub>H<sub>2</sub>. (energies in eV, isovalue = 0.02)

	LUMO	HOMO	HOMO-LUMO (HCl→Au <sub>n</sub> -C <sub>2</sub> H <sub>2</sub> )	HOMO-LUMO (Au <sub>n</sub> -C <sub>2</sub> H <sub>2</sub> →HCl)
HCl	-0.81	-9.19		
Au <sub>3</sub> -C <sub>2</sub> H <sub>2</sub>	-3.57	-5.00	5.62	4.19
Au <sub>4</sub> -C <sub>2</sub> H <sub>2</sub>	-2.98	-5.96	6.21	5.14
Au <sub>5</sub> -C <sub>2</sub> H <sub>2</sub>	-3.95	-5.24	5.24	4.42
Au <sub>6</sub> -C <sub>2</sub> H <sub>2</sub>	-2.94	-6.29	6.25	5.48
Au <sub>7</sub> -C <sub>2</sub> H <sub>2</sub>	-4.40	-5.51	4.79	4.69
Au <sub>8</sub> -C <sub>2</sub> H <sub>2</sub>	-3.38	-6.24	5.81	5.42
Au <sub>9</sub> -C <sub>2</sub> H <sub>2</sub>	-4.29	-5.34	4.91	4.52
Au <sub>10</sub> -C <sub>2</sub> H <sub>2</sub>	-3.71	-5.86	5.48	5.05

Table 2. The chemical bonds for increase (%) of  $R_{C\equiv C}$  ( $C_2H_2$ ) and  $R_{H-Cl}$  (HCl) in  $Au_n-C_2H_2-HCl$  complexes.

	$Au_3$	$Au_4$	$Au_5$	$Au_6$	$Au_7$	$Au_8$	$Au_9$	$Au_{10}$
$R_{C\equiv C}$	2.42	2.56	1.99	1.03	1.54	1.22	1.23	1.32
$R_{H-Cl}$	3.29	2.67	3.61	1.02	2.55	0.96	1.40	2.71